Carbon Powders Prepared by Ultrasonic Spray Pyrolysis of Substituted Alkali Benzoates†

Sara E. Skrabalak and Kenneth S. Suslick*

Department of Chemistry, University of Illinois at Urbana-Champaign, 600 South Mathews Avenue, Urbana, Illinois 61801

Received: February 13, 2007; In Final Form: April 13, 2007

Ultrasonic spray pyrolysis (USP) has been used to prepare carbon spheres from aqueous solutions of substituted alkali benzoate salts. The size of the carbon spheres produced during USP can easily be controlled simply by changing the concentration of the precursor solution. Both the cation and the ring substituents of a given precursor influence product morphology, which ranges from solid spheres to hollow bowls to porous spheres. Thermogravimetic analysis of the various precursors suggests that the relative temperature of decomposition steps releasing gas explain these observed morphology differences.

Introduction

Since the discovery of C_{60} by Smalley, Kroto, and Curl in 1985,[1] there has been a sustained interest in the large-scale production of carbon materials with controlled morphologies.[2−4] The production of carbon spheres (with or without pores) has been of particular interest for use as lithium battery anodes, column packing materials for separations, selective absorbents, lightweight composite components, and catalyst supports.[5−10] The synthetic methods developed thus far rely on either laborious multistep methods (e.g., templating techniques or surfactant-stabilized emulsion polymerizations followed by carbonization and separations)[5,11−14] or simpler direct hydrocarbon pyrolysis methods.[15−18] While the former methods are potentially cost and scale prohibitive, the later methods for sphere formation are experimentally simple but also potentially dangerous, especially on the large-scale, because of precursor flammability. Safer precursors that are compatible with direct pyrolysis methods are desirable; however, such precursors typically have low volatility thus limiting their utility.

Ultrasonic spray pyrolysis (USP) is well-suited for the continuous production of spherical particles from low-volatility precursors,[19−21] eliminating many of the safety concerns that arise from the hydrocarbon pyrolysis techniques. With USP, ultrasound is used to produce precursor solution droplets dispersed in a carrier gas. As these aerosol droplets are then heated, solvent evaporation and precursor decomposition occurs, generating product, generally with spherical morphology. With low volatility precursors, the reactions responsible for product formation are confined within the individual droplets. In this way, the droplets formed during USP act as individual submicrometer-sized chemical reactors that impose morphology control on the products. Additionally, since one droplet can produce one particle, simply changing the concentration of the precursor solution will change the size of the particle produced.[22−24]

There are numerous examples of inorganic materials (e.g., metal oxides and sulfides) being produced as fine powders from USP of metal salt containing solutions (e.g., typically, metal nitrates, chlorides, or acetates).[19−21] There is, however, very little work on the production of carbon materials using USP. In 2006, we reported the synthesis of porous carbon networks from USP of aqueous solutions containing nonaromatic alkali carboxylates (e.g., alkali chloroacetates and alkali dichloroacetates).[25] Here, we report the use of substituted alkali benzoates as carbon precursors for USP. In general, carbon spheres are produced, with varying degrees of porosity being observed depending on the precursor.

Experimental Section

USP Apparatus. The USP experimental setup has been described elsewhere in more detail.[26−28] In brief, the base of a Sunbeam 1.7 MHz household humidifier was used to nebulize a precursor solution into a fine mist. The generated mist was then carried by an argon flow (∼1 slpm) into a furnace (700 °C), and products were collected in water-filled bubblers at the furnace outlet. A schematic of this setup is shown in Supporting Information Figure 1.

Materials. 3,5-dihydroxybenzoic acid (purity 97%), 1,3,5-benzenetricarboxylic acid (purity 98%), 4-chlorobenzoic acid (purity 99%), 2-chlorobenzoic acid (purity 98%), 3-hydroxybenzoic acid (purity 99%), 3,4-dichlorobenzoic acid (purity 99%), 1,2,4,5-benzenetetracarboxylic acid (purity 96%), terephthalic acid (purity 98%), 4,5-dihydroxy-1,3-benzene disulfonic acid disodium salt monohydrate, trimesic acid, 2,5-dichloro-3-nitrobenzoic acid (purity 98%), gallic acid, benzoic acid (purity 99.5%), and 2,3,4 trihydroxybenzoic acid were purchased from Aldrich and used as received. 3,5-dichloro-4-hydroxybenzoic acid (purity 97%), 3,5-dichloro-2-hydroxybenzene sulfonic acid sodium salt (purity 99%), and 2,4,6-trichlorobenzoic acid (purity 94%) were purchased from Alfa Aesar and used as received. 2,5-dichloroterephthalic acid (purity 97%) and mellitic acid (purity 96%) were purchased from TCI and used as received.

Precursor Solution Preparation. Precursor solutions were prepared by first dissolving or suspending the acid of a particular precursor in an appropriate amount of water. The corresponding amount of alkali hydroxide then was added to completely deprotonate the acid. Agitation or heating was often required to produce a homogeneous solution of a desired concentration. Volumetric methods were employed.

Product Isolation. USP products were isolated from the collection media by centrifugation with the aid of centrifugal

† Part of the special issue "Richard E. Smalley Memorial Issue".

* Corresponding author. E-mail: ksuslick@uiuc.edu.

10.1021/jp071241x CCC: $37.00
Published on Web 07/03/2007

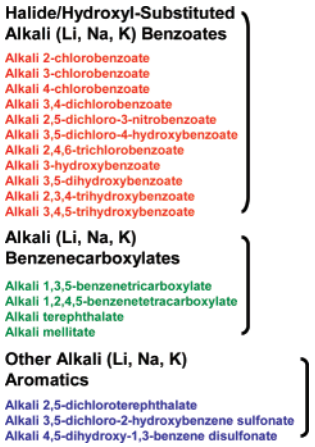

Figure 1. List of substituted alkali benzoate precursors that produce carbon spheres via USP at 700 °C.

filters. The products were washed with purified water (a minimum of three times) and vacuum dried at ~80 °C for 12 h prior to analysis.

Thermogravimetric Analysis (TGA). Solid powders of the precursors were isolated by rotary evaporation followed by vacuum drying prior to analysis. TGA was conducted with a calibrated Mettler Toledo TGA/SDTA851e at ambient pressure with a flow of N_2 gas (20 sccm). Ceramic crucibles were used as sample holders (sample mass: 10 to 20 mg). Samples were analyzed at a scan rate of 10°/min.

Characterization of Carbon Materials. A scanning electron microscope (Hitachi S4700 SEM operating between 10 and 15 kV) was used to observe sample morphology. Bulk elemental analysis was conducted by the Microanalysis Laboratory at the University of Illinois at Urbana−Champaign. Powder X-ray diffraction (XRD) was conducted with a Rigaku D-MAX system using Cu Kα radiation; operating conditions were 45 kV and 20 mA.

Results and Discussion

Precursor Survey. A complete list of the substituted alkali benzoates studied is shown in Figure 1; it is divided into 3 categories: halide/hydroxyl substituted alkali benzoates, alkali benzenecarboxylates, and other alkali aromatics (i.e., hybrid precursors or sulfonates). Interestingly, all of the precursors listed in Figure 1 produced carbon materials with well-defined sphere-like morphologies. In contrast, USP of unsubstituted alkali benzoate solutions produced little carbonaceous material except at high solution concentrations (e.g., [sodium benzoate] > 1 M), and even then, only ill-defined carbon solids were produced (in addition to alkali carbonate). Presumably, during pyrolysis, substituted benzoates provide more reactive intermediates or more sites for reactivity than unsubstituted benzoates.

Additionally, USP at 700 °C of neat benzene and chlorobenzene produced no carbonaceous solids although a slight discoloration was observed in the collected chlorobenzene product. While soot formation from such precursors is well-documented,[29−31] under our USP conditions, it appears that either the temperature was too low or the residence time was too short for an efficient reaction. Alternatively, while these hydrocarbons are delivered to the heated zone as a liquid droplet, they are rapidly heated, making evaporation from the droplets quick. In this way, the local concentration of benzene or chlorobenzene might be too low to promote large, nonvolatile hydrocarbon formation. Regardless of the reason, carbon materials are not produced from USP of benzene and chlorobenzene.

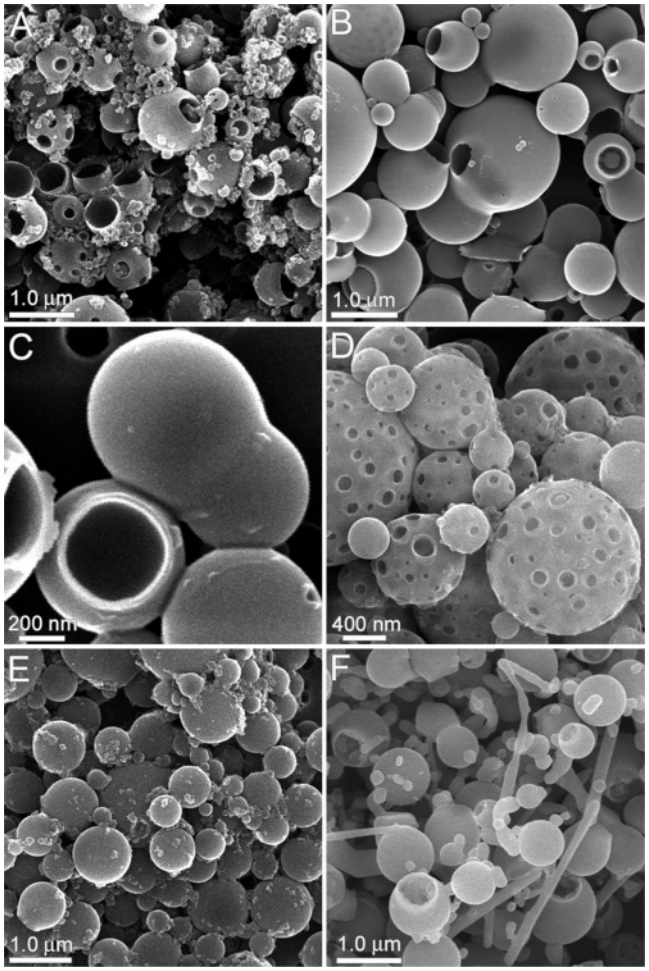

Figure 2. SEMs of USP products from 0.25 M aqueous solutions of (A) sodium 2-chlorobenzoate, (B) sodium 3-chlorobenzoate, (C) sodium 4-chlorobenzoate, (D) lithium 3-chlorobenzoate, and (E) potassium 3-chlorobenzoate. (F) An SEM of the unwashed sodium 3-chlorobenzoate product; after washing, the solid particulates and the longer strands dissolve, as seen in (B).

Electron Microscopy. Scanning electron microscopy (SEM) images of the USP products from select substituted alkali benzoate and alkali benzenecarboxylate solutions are shown in Figures 2 and 3. In general, carbon spheres are produced. In some cases, the spheres are solid; in others, large holes or hollows are observed in the materials creating a bowl-like morphology, and in yet others, the spheres are intact, but porous. An explanation for these differences will be developed later.

Shown in Figure 4 is a representative SEM image (Figure 4A) of the USP product from sodium 3-hydroxybenzoate as well as a plot of the average sphere volume as a function of solution concentration (Figure 4B). Interestingly, a linear relationship is observed which is consistent with modifications to the Lang equation (eq 1 below), which describes the diameter of droplets generated by ultrasonic nebulization as a function of solution properties and atomization frequency.[19] When the solution concentration and properties of the generated product are known, the diameter of the generated product can be approximated, as shown in eq 2, which can be reformulated to describe the particle volume (assuming spherical particles) as is shown in eq 3: the volume of the generated solid particle, V_p, is directly proportional to the solution concentration, C_s. Even though the size distribution is broad (primarily because of the droplet coalescence in our simple apparatus, which is

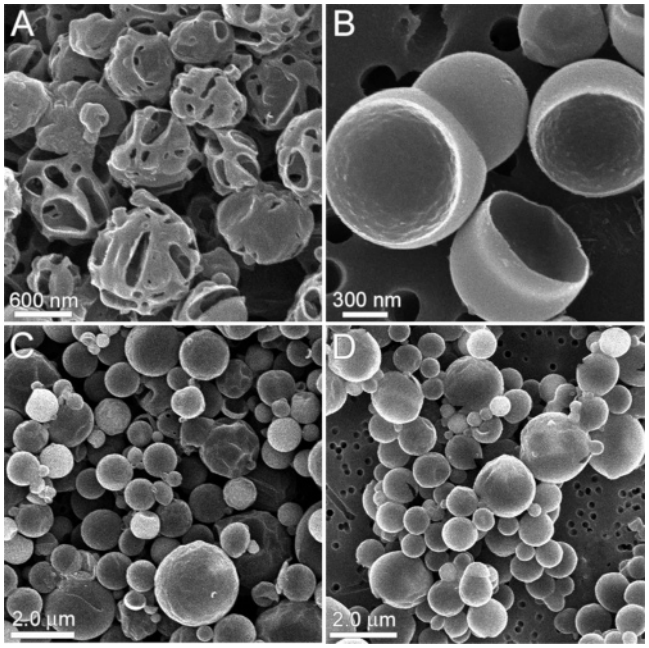

Figure 3. SEMs of USP products from alkali benzenecarboxylate solutions: (A) 0.125 M sodium terephthalate, (B) 0.125 M sodium 1,3,5-benzenetricarboxylate, (C) 0.25 M sodium 1,2,4,5-benzenetetracarboxylate, and (D) 0.125 M sodium mellitate.

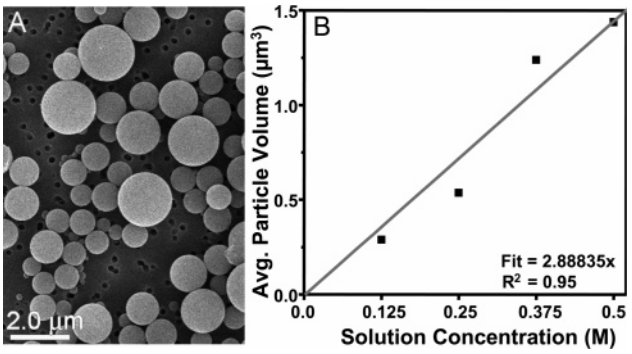

Figure 4. (A) SEM of USP product from a 0.375 M sodium 3-hydroxybenzoate solution. (B) Plot of the mean carbon particle volume as a function of sodium 3-hydroxybenzoate solution concentration (each sample, $N \approx 250$ particles); best-fit line is in gray.

not optimized for uniform particle size production), the results shown in Figure 4 confirm that the carbon sphere size can be directly controlled by simply changing the solution concentration.[22]

$$D_d = 0.34\left(\frac{8\pi\sigma}{\rho f^2}\right)^{1/3} \quad (1)$$

D_d = droplet diameter, σ = surface tension, ρ = density, and f = atomization frequency.

$$D_p = \left(\frac{MD_d{}^3C_s}{1000\rho}\right)^{1/3} \quad (2)$$

D_p = particle diameter, M = molecular weight, C_s = molar concentration, D_d = droplet diameter, and ρ = density.

$$V_p = \frac{4\pi MD_d{}^3C_s}{3000\rho} \quad (3)$$

V_p = particle volume, M = molecular weight, C_s = molar concentration, D_d = droplet diameter, and ρ = density.

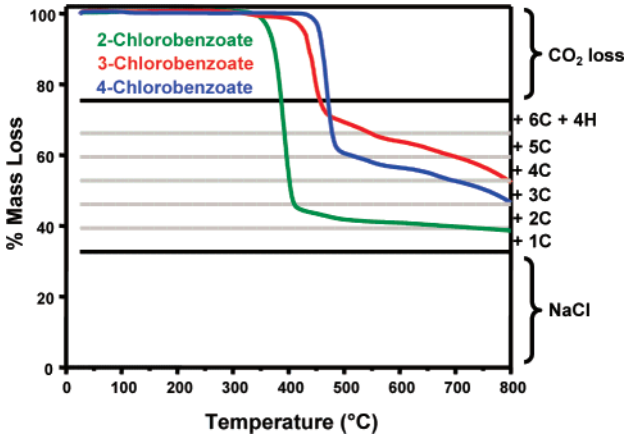

Figure 5. TGA of sodium 2-, 3-, and 4-chlorobenzoate.

Electron micrographs of the unwashed products indicate the formation of a water-soluble product, presumably salt, in addition to carbon material (Figure 2F). In contrast to our previous work, the generated salt, however, does not clog the holes of the carbon materials. This difference is likely related to the thermal properties of the various benzoate precursors and suggests that the mechanism for pore or bowl formation is different from our previous work with the simple alkali halocarboxylates in which generated salts act as porogens during carbon network formation.

X-ray Powder Diffraction. XRD of the unwashed USP products (and thermally decomposed precursors) supports the formation of soluble salts during pyrolysis. For example, XRD of the unwashed sodium benzenecarboxylate pyrolysis products indicates sodium carbonate formation (Supporting Iinformation, Figure 2A), while NaCl formation is indicated from the pyrolysis of sodium 2-, 3-, and 4-chlorobenzoate, although some sodium carbonate is also indicated as a contaminant (Supporting Information, Figure 2B). In general, the corresponding alkali carbonate is generated during pyrolysis of alkali benzenecarboxylates or hydroxyl-substituted alkali benzoates, and the corresponding alkali halide is produced from pyrolysis of halide-substituted alkali benzoates.[32−36] Work by Bandosz and coworkers[36] indicates the formation of metal sulfates and sulfides, from the pyrolysis of metal sulfonates, and the release of SO_2.

No other features were observed in the XRD patterns of the unwashed samples, and washing the samples removed the generated salts completely. The amorphous material was primarily carbon (e.g., ~80 wt % C for the sodium 3-chlorobenzoate and sodium 3-hydroxybenzoate USP products determined by bulk elemental analysis), with substantial oxygen (~15 wt % O by difference). Heat treatment (900 °C, helium 30 sccm, 12 h) of the various powders did not induce crystallization and suggests that the reactive growth species primarily responsible for sphere formation are not aromatic in nature.

Thermogravimetric Analysis. Thermogravimetric analyses of selected precursors were conducted to elucidate the mechanism of salt and carbon material formation. Here, various alkali chlorobenzoate precursors will be considered. While many other substituted benzoates produced carbon spheres (Figure 1), their decomposition behaviors were much more complex, making interpretation difficult.

Shown in Figure 5 are the TGA results for sodium 2-, 3-, and 4-chlorobenzoate. Sodium 2-chlorobenzoate displayed a single concerted mass loss at ~400 °C. In contrast, sodium 3- and 4-chlorobenzoate displayed concerted mass losses at ~450 and ~470 °C, respectively, followed by gradual secondary losses

immediately thereafter. These observations suggest that sodium 2-chlorobenzoate follows a decomposition mechanism different from that of sodium 3- and 4-chlorobenzoate. As sodium 2-chlorobenzoate decomposes in a concerted manner to produce NaCl, the most likely initial product is *o*-benzyne. Köbrich,[37] Kochi,[38] and McNelis[39] have studied the pyrolysis of *o*-halobenzoates, and from their work, direct evidence for the formation of *o*-benzyne, as a reactive intermediate, was obtained via mass spectrometry and trapping experiments. Assuming complete NaCl formation from the pyrolysis of sodium 2-chlorobenzoate, ~10% of the initial mass remains, corresponding to approximately one carbon atom. This result suggests that *o*-benzyne, while formed, is not likely responsible for carbon sphere formation. Rather, the majority of the generated *o*-benzyne, being highly volatile, likely evaporates from the heated droplets, while approximately one in six sodium 2-chlorobenzoate units (corresponding to the unaccounted for carbon) are involved in carbon sphere formation. Thus, carbon sphere formation could proceed through reactions of trapped *o*-benzyne moieties with either precursor or other *o*-benzyne molecules. Alternatively, the competing reaction responsible for sodium carbonate formation could be responsible for carbon sphere formation.

The TGA results from sodium 3- and 4-chlorobenzoate are more complex; work by Berry and co-workers[40−42] as well as Fisher and Lossing[43] on the photolysis/pyrolysis of *m*- and *p*-substituted compounds suggests that these precursors could decompose through *m*- and *p*-benzyne intermediates.[44] Assuming complete decarboxylation and NaCl formation, we find that volatile species (e.g., *m*- or *p*-benzyne, among others) must be produced, as indicated by the concerted mass losses at ~450 °C (Figure 5). Significantly, much more of the original masses remain after the first decomposition process (excluding mass from NaCl formation, ~35% and 25% for sodium 3- and 4-chlorobenzoate, respectively) than was observed for the pyrolysis of sodium 2-chlorobenzoate; this difference is likely due to the much greater reactivity of the intermediates (i.e., *m*- and *p*-benzyne compared to *o*-benzyne) produced from the pyrolysis of sodium 3- and 4-chlorobenzoate. It is the byproducts from these reactive species (i.e., possibly hex-3-ene-1,5-diyne or vinylidene) that are responsible for carbon sphere formation. The observed secondary losses are likely due to the release of small volatile hydrocarbons such as acetylene, generated during carbon sphere consolidation and cross-linking reactions.

An interesting observation can also be made upon closer examination of the SEM images of the USP products from sodium 2-, 3-, and 4-chlorobenzoate (Figure 2A−C). In general, all three precursors yield spheres of similar morphology. The sodium 2-chlorobenzoate product, however, displays a bimodal distribution; in addition to the micrometer-sized carbon spheres, nanosized carbon debris is observed (Figure 2A). Bimodal distributions arise from USP when precursors with widely different volatilities are employed in the same synthesis. The above proposal, in which the highly volatile but slightly more stable *o*-benzyne is produced from sodium 2-chlorobenzoate but is not produced from sodium 3- and 4-chlorobenzoate, is consistent with these SEM observations. Once released from the reaction droplet, the diffuse *o*-benzyne molecules react in the gas phase to produce the nanosized carbon debris (Interestingly, the potassium 2-chlorobenzoate USP product also displays a bimodal distribution while the USP product of potassium 3- and 4-chlorobenzoate do not.)

TGA was also conducted on lithium and potassium 3-chlorobenzoate and compared with that of sodium 3-chlorobenzoate (Figure 6). Notice that both sodium and potassium 3-chlorobenzoate display similar decomposition pathways, with a single concerted mass loss. Lithium 3-chlorobenzoate, however, displays different behavior, undergoing two mass losses: one at ~200 °C and a second at ~450 °C. Interestingly, the USP product from lithium 3-chlorobenzoate displays a distinctly different morphology in which the spheres produced contain numerous holes (Figure 2D). In contrast, the products from sodium and potassium 3-chlorobenzoate are primarily bowl-like, containing a single large hole (Figure 2B,E). These observations suggest that holes are formed from the gaseous blow-out of volatile species produced during cross-linking (i.e., lower temperature (early) decomposition as observed with lithium 3-chlorobenzoate) or after full cross-linking (i.e., higher temperature (later) decomposition as observed with sodium and potassium 3-chlorobenzoate). It appears, therefore, that the precursor decomposition behavior is primarily responsible for observed morphology differences: gaseous products produced early in the decomposition, (e.g., water of crystallization at 100 to 300 °C, small hydrocarbons at variable temperatures, and CO_2 from nonaromatic carboxylates at 150 to 300 °C, as determined by TG-MS) produce porous spheres, whereas such products produced later in the cross-linking process (e.g., CO_2 and CO from aromatic carboxylates or carboxyls at >400 °C as determined by thermogravimetry-mass spectroscopy, TG-MS) create bowl-like morphologies.[33,45]

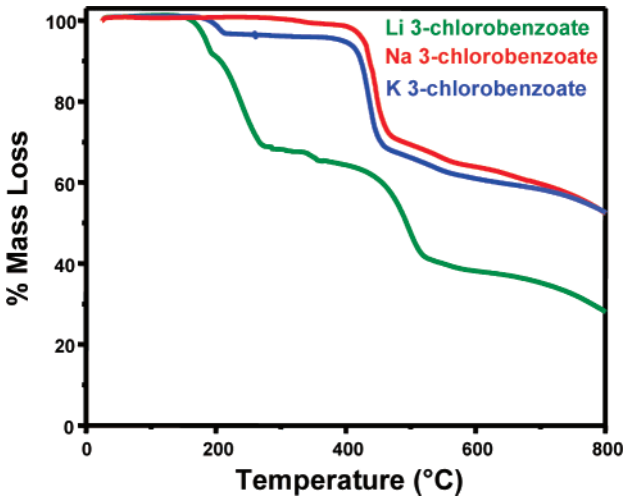

Figure 6. TGA of lithium 3-chlorobenzoate (green), sodium 3-chlorobenzoate (red), and potassium 3-chlorobenzoate (blue).

Conclusions

We find that aqueous solutions of substituted alkali benzoates can be used as precursors for the generation of carbon spheres using ultrasonic spray pyrolysis, with morphologies ranging from solid spheres to hollow bowls to porous spheres. Unlike previous methods for sphere formation, the USP method uses aqueous solutions of nonflammable precursors for the quick and continuous generation of particles with controlled sizes and morphology.

Acknowledgment. These studies were supported by the NSF (CHE0315494) with characterizations carried out in the Center for Microanalysis of Materials, UIUC, which is partially supported by the U.S. DOE under Grant DEFG02-91-ER45439.

Supporting Information Available: Schematic of the USP setup and additional materials characterizations (XRD). This material is available free of charge via the Internet at http://pubs.acs.org.

References and Notes

(1) Kroto, H. W.; Heath, J. R.; Obrien, S. C.; Curl, R. F.; Smalley, R. E. *Nature* **1985**, *318*, 162.

(2) Pierson, H. O. *Handbook of Carbon, Graphite, Diamond, and Fullerenes: Properties, Processing and Applications*; Noyes Publications: Park Ridge, NJ, 1993; p 405.

(3) Xia, Y. N.; Yang, P. D.; Sun, Y. G.; Wu, Y. Y.; Mayers, B.; Gates, B.; Yin, Y. D.; Kim, F.; Yan, Y. Q. *Adv. Mater.* **2003**, *15*, 353.

(4) Delhaes, P.; Kuzmany, H. *Fullerenes and Carbon Based Materials;* Elsevier Science: Lausanne, Switzerland, 1998; p 376.

(5) Lee, J.; Kim, J.; Hyeon, T. *Adv. Mater.* **2006**, *18*, 2073.

(6) Marsh, H.; Reinoso, F. R. *Activated Carbon*; Elsevier Ltd.: Oxford, England, 2006; p 554.

(7) Zheng, T.; Liu, Y. H.; Fuller, E. W.; Tseng, S.; Vonsacken, U.; Dahn, J. R. *J. Electrochem. Soc.* **1995**, *142*, 2581.

(8) Jones, C. W.; Koros, W. J. *Carbon* **1994**, *32*, 1419.

(9) De Jong, K. P.; Geus, J. W. *Catal. Rev. Sci. Eng.* **2000**, *42*, 481.

(10) Moreno-Castilla, C.; Maldonado-Hodar, F. J. *Carbon* **2005**, *43*, 455.

(11) Jang, J.; Ha, H. *Chem. Mater.* **2003**, *15*, 2109.

(12) Jang, J.; Lim, B. *Adv. Mater.* **2002**, *14*, 1390.

(13) Tosheva, L.; Parmentier, J.; Valtchev, V.; Vix-Guterl, C.; Patarin, J. *Carbon* **2005**, *43*, 2474.

(14) Kocirik, M.; Brych, J.; Hradil, J. *Carbon* **2001**, *39*, 1919.

(15) Jin, Y. Z.; Gao, C.; Hsu, W. K.; Zhu, Y.; Huczko, A.; Bystrzejewski, M.; Roe, M.; Lee, C. Y.; Acquah, S.; Kroto, H.; Walton, D. R. M. *Carbon* **2005**, *43*, 1944.

(16) Pol, V. G.; Pol, S. V.; Calderon-Moreno, J. M.; Gedanken, A. *Carbon* **2006**, *44*, 3285.

(17) Qian, H.; Han, F.; Zhang, B.; Guo, Y.; Yue, J.; Peng, B. *Carbon* **2004**, *42*, 761.

(18) Xia, Y.; Mokaya, R. *Adv. Mater.* **2004**, *16*, 886.

(19) Kodas, T. T.; Hampden-Smith, M. J. *Aerosol Processing of Materials*; Wiley-VCH: New York, 1999; p 680.

(20) Messing, G. L.; Zhang, S. C.; Jayanthi, G. V. *J. Am. Ceram. Soc.* **1993**, *76*, 2707.

(21) Patil, P. S. *Mater. Chem. Phys.* **1999**, *59*, 185.

(22) Okuyama, K.; Lenggoro, I. W.; Tagami, N.; Tamaki, S.; Tohge, N. *J. Mater. Sci.* **1997**, *32*, 1229.

(23) Xia, B.; Lenggoro, I. W.; Okuyama, K. *Adv. Mater.* **2001**, *13*, 1579.

(24) Didenko, Y. T.; Suslick, K. S. *J. Am. Chem. Soc.* **2005**, *127*, 12196.

(25) Skrabalak, S. E.; Suslick, K. S. *J. Am. Chem. Soc.* **2006**, *128*, 12642.

(26) Skrabalak, S. E.; Suslick, K. S. *J. Am. Chem. Soc.* **2005**, *127*, 9990.

(27) Suh, W. H.; Suslick, K. S. *J. Am. Chem. Soc.* **2005**, *127*, 12007.

(28) Suh, W. H.; Jang, A. R.; Suh, Y.-H.; Suslick, K. S. *Adv. Mater.* **2006**, *18*, 1832.

(29) Wiersum, U. E.; Jenneskens, L. W. The Formation of Polyaromatic Hydrocarbons, Fullerenes, and Soot in Combustion: Pyrolytic Mechanisms and the Industrial and Environmental Connection. In *Gas-phase Reactions in Organic Synthesis*; Vallee, Y., Ed.; Overseas Publishers Association: Amsterdam, The Netherlands, 1997; p 143.

(30) Hurd, C. D. *Pyrolysis of Carbon Compounds*; Chemical Catalogue Co.: New York, 1929.

(31) Fields, E. K.; Meyerson, S. *Acc. Chem. Res.* **1969**, *2*, 273.

(32) Hu, G.; Ma, D.; Cheng, M.; Liu, L.; Bao, X. *Chem. Commun.* **2002**, 1948.

(33) Kamegawa, K.; Kodama, M.; Nishikawa, K.; Yamada, H.; Adachi, Y.; Yoshida, H. *Microporous Mesoporous Mater.* **2005**, *87*, 18.

(34) Hites, R. A.; Biemann, K. *J. Am. Chem. Soc.* **1972**, *94*, 5772.

(35) Dabestani, R.; Britt, P. F.; Buchanan, A. C., III. *Energy Fuels* **2005**, *19*, 36.

(36) Hines, D.; Bagreev, A.; Bandosz, T. J. *Langmuir* **2004**, *20*, 3388.

(37) Kobrich, G. *Chem. Ber.* **1959**, *92*, 2985.

(38) Kochi, J. K. *J. Org. Chem.* **1961**, *26*, 932.

(39) McNelis, E. *J. Org. Chem.* **1963**, *28*, 3188.

(40) Berry, R. S.; Spokes, G. N.; Stiles, M. *J. Am. Chem. Soc.* **1962**, *84*, 3570.

(41) Berry, R. S.; Clardy, J.; Schafer, M. E. *Tetrahedron Lett.* **1965**, *15*, 1003.

(42) Berry, R. S.; Clardy, J.; Schafer, M. E. *Tetrahedron Lett.* **1965**, *15*, 1011.

(43) Fisher, I. P.; Lossing, F. P. *J. Am. Chem. Soc.* **1963**, *85*, 1018.

(44) Sander, W. *Acc. Chem. Res.* **1998**, *32*, 669.

(45) Shimanouchi, N. *Thermochim. Acta* **1983**, *62*, 221.